Dalton Transactions

An international journal of inorganic chemistry

www.rsc.org/dalton

Volume 41 | Number 9 | 7 March 2012 | Pages 2529–2836

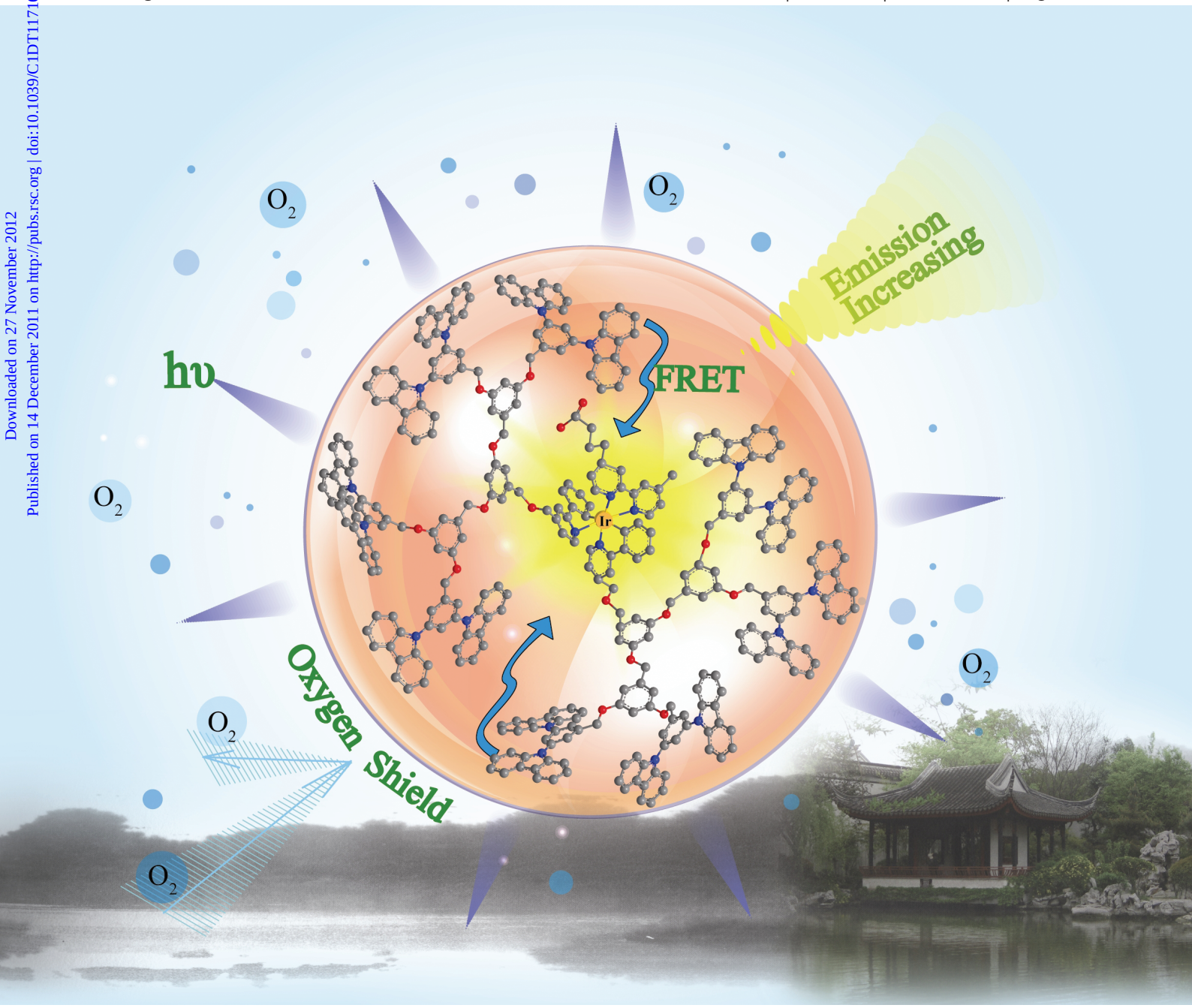

ISSN 1477-9226

RSC Publishing

COVER ARTICLE

Li, Liu and Zhou

Synthesis and properties of a dendritic FRET donor–acceptor system with cationic iridium(III) complex core and carbazolyl periphery

Dalton Transactions

Dynamic Article Links
View Article Online

Cite this: *Dalton Trans.*, 2012, **41**, 2582

www.rsc.org/dalton

PAPER

Synthesis and properties of a dendritic FRET donor–acceptor system with cationic iridium(III) complex core and carbazolyl periphery†

Yanfang Li,[a,b] Yang Liu*[a,c] and Ming Zhou*[a,c]

Received 10th September 2011, Accepted 8th November 2011
DOI: 10.1039/c1dt11716e

In order to enhance the photoluminescence of cyclometalated iridium(III) complexes, which are potentially useful for biolabeling and bioimaging, a series of benzyl ether branched dendritic moieties with carbazolyl termini were introduced to the cyclometalating *C^N* ligands of the heteroleptic Ir(III) complexes. The complexes also contain a bidentate bipyridine ligand with a carboxyl group for further bioconjugation or functionalization. The dendritic benzyl ether moieties with carbazolyl peripheral groups have demonstrated a dual function as both a Förster resonance energy transfer (FRET) donor and an oxygen shield to the Ir(III) complex core. The peripheral carbazolyl groups absorb UV light more intensively and transfer energy efficiently to the Ir(III) complex core *via* the FRET effect, and thus the photoluminescence of the Ir(III) complex at around 560 nm is significantly enhanced. Furthermore, the benzyl ether dendrimers containing carbazolyl termini can shield the Ir(III) complex core to weaken the oxygen quenching effect, which leads to a further enhancement of the PL of the Ir(III) complex.

Introduction

Transition metal complexes, such as Ir(III), Ru(II), Os(II) and Re(I) complexes, are characterized by their metal to ligand change transfer (MLCT) transition leading to phosphorescent emission. Among them, cyclometalated iridium(III) complexes are of special interest as promising photoluminescent (PL) substances widely used as dopants for organic light-emitting diodes (OLEDs),[1–8] luminescent bio-labeling reagents,[9–16] photocatalysis[17] and chemosensors for oxygen,[18–21] heavy metal ions,[22–25] anions[26–28] and amino acids.[29,30] In addition to the general features of transition metal complexes, such as the long lifetime of the excited state and the large Stokes shift for easy separation of excitation and emission wavelengths, cyclometalated Ir(III) complexes normally have high photochemical stability due to the chelating bonds of the cyclometalating ligands with the metal atoms, high quantum efficiencies[31,32] and a broad range of tunability[33,34] of emission properties that allow their luminescence to span from NIR to blue light. The largely tunable photophysical properties of Ir(III) complexes have been realized by varying the ligands of either the homoleptic or heteroleptic Ir(III) complexes. In addition, the Ir(III) complexes can be made electrically negative (anionic[35]), neutral and positive (cationic complexes[36]), offering versatile application possibilities.

In biological and medical fields, ruthenium(II) polydiimine complexes and lanthanide (Eu(III), Tb(III) *etc.*) cryptates have been successfully used as bio-labels in commercial electrochemiluminescence[37] and time-resolved fluorescence immunoassays,[38,39] respectively. Interest in developing luminescent metal complexes and exploiting their bio-applications has grown rapidly since the successful industrial introduction of metal complex-based bio-analytical methodologies. Cyclometalated Ir(III) complexes are among the most important families of these complexes, which may potentially be developed to a level of commercial value.[40] It has been reported that the luminescence from Ir(III) complexes can be generated by both photo-excitation and electrochemical excitation.[41] Luminescence generated by photon excitation is simpler in some applications but often suffers from insufficient absorption cross section, even though the quantum yields are acceptably high. A mechanism of enhancing the absorption and thus the emission of luminophores is to utilize Förster resonance energy transfer (FRET),[42] by which a donor, which has a large absorption extinction coefficient, absorbs light energy and efficiently transfers the energy to the nearby acceptor, which then becomes excited and emits luminescence (*i.e.*, the signal of detection value).

It was our objective in this work to construct such a system in Ir(III) complexes, the applications of which have been largely biased towards OLEDs so far, to demonstrate the intramolecular energy transfer that helps to gain more intense emission from the luminophores. A strategy of introducing as many donor moieties as possible has been demonstrated through the design and the

[a]*Suzhou Institute of Nano-Tech and Nano-Bionics, Chinese Academy of Sciences, 398 Ruoshui Road, Suzhou Industrial Park, Jiangsu, 215123, P. R. China. E-mail: mzhou2007@sinano.ac.cn, yliu2007@sinano.ac.cn; Fax: +86-512-62872181; Tel: +86-512-62872558*
[b]*Graduate School of the Chinese Academy of Sciences, Beijing, 100049, P. R. China*
[c]*SunaTech Inc. bioBAY, Suzhou Industrial Park, Jiangsu, 215123, P. R. China*

†Electronic supplementary information (ESI) available: Extra absorption, emission, ^{1}H and ^{13}C NMR and mass spectra, and cyclic voltammograms. See DOI: 10.1039/c1dt11716e

successful syntheses of a series of dendritic scaffolds (Scheme 1). The donor used in this work is the carbazolyl group, which possesses well studied photo- and electrochemical properties, such as relatively intense luminescence[43] and reversible oxidation processes.[44] The energy level of the emission of carbazole (~360 nm) matches well with the MLCT absorption bands of many Ir(III) complexes.[45–48] As perfectly branched polymeric moieties with a high density of surface functionalizable sites, the dendritic scaffolds used in the FRET molecular structures are not novel.[49,50] The introduction of dendrimers into metal complexes was first reported by Serroni *et al.*[51] in 1994. It is worth noting that Li *et al.* have synthesized Ir(III)-cored dendrimers with carbazole peripherally functionalized β-diketone dendritic ligands and observed remarkable FRET phenomena.[45] Introducing the FRET donors to the β-diketonato ligand provides a strategy for easily synthesizing a large number of Ir(*C^N*)$_2$(acac), which could share the carbazole functionalized β-diketonato. Similarly, Kwon and coworkers reported dendrimer light-harvesting systems and a high intramolecular energy transfer efficiency greater than 90% based on FIrpic (iridium(III)bis[(4,6-difluorophenyl)pyridinato-*N*,$C^{2'}$]picolinate) with dendritic picolinate ligands containing carbazolyl peripheral groups.[46] This system was further modified to include a biotin functional group for potential bioanalytical application.[48]

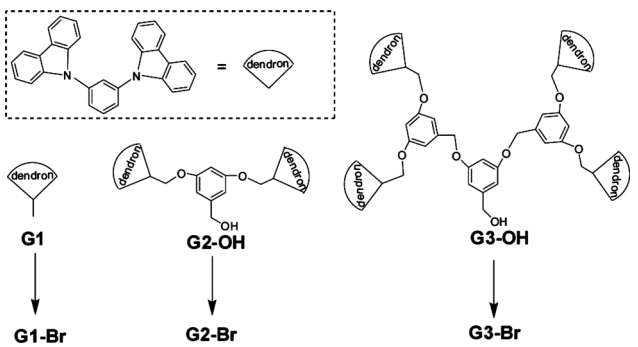

Scheme 1 Dendritic donor precursors.

In the above mentioned work, the donor moieties at the dendritic peripheries are built on just one ligand, *i.e.*, the ancillary ligand of the heteroleptic Ir(III) complexes. We intended to introduce more donor groups without having to extend the branch lengths or to increase the number of the dendrimer generation. Most importantly, we intended to build a system with a bio-conjugatable capability based on the usual amide chemistry, as it is generally employed in bio-labeling and bio-conjugation techniques.[52] Therefore, unlike other previous systems, the donor-bearing dendritic scaffolds were based on the two cyclometalating *C^N* ligands, rather than the heteroleptic ancillary ligand, such as acac[45] and picolinate.[46] This strategy of introducing more donors could be more synthetically challenging than in the cases of dendronizing acac or picolinate, because the bulky dendronized *C^N* ligand make the cyclometalation reaction during the Ir(III) dimer formation more difficult. In addition, the Ir(III) compounds in this work have a positive charge (cationic luminophores) due to the charge imbalance arising from replacement one of the usual carbon–metal bonds (between the iridium(III) and the *C^N* ligands) with the coordination bonds (between the metal and the bio-conjugatable diimine ligand). Such a bio-conjugatable system provides possibilities for further applications that require covalent incorporation of the luminophores with biomolecules, a target recognizable moiety or other biologically active substances.

Reported here are the synthesis and properties of a series of cationic bis-cyclometalated Ir(III) complex (acceptor) cored bio-conjugatable compounds having peripheral carbazolyl moieties (donor) and a carboxylic acid functionalized bipyridine (*N^N* ligand) derivative as an ancillary ligand. The compounds of different generations of dendritic scaffolds contain 0, 4, 8 and 16 carbazolyl groups. The photophysical properties and the emission enhancement as combined results of both the FRET and the dendrimer shielding effect on oxygen quenching will be discussed.

Results and discussion

Synthesis and characterization

Dendritic donor precursors (**G1-Br**, **G2-Br**, and **G3-Br**) were prepared by the convergent strategy according to the literature[46] (Scheme 1). Phenylpyridine (ppy) derivatives, (2-phenylpyridin-4-yl)methanol (**4**) and (4-(pyridin-2-yl)phenyl)methanol (**8**), were synthesized from 4-methyl-2-phenylpyridine (**1**) and 2-*p*-tolylpyridine (**5**) (Scheme 2). Conjugation of benzyl bromide of the dendritic donor precursors with the benzyl alcohol groups of **4** and **8** gave dendritic *C^N* ligands, $\boldsymbol{L_{Gn}}$ and $\boldsymbol{L_{Gn}'}$, respectively (Scheme 3).

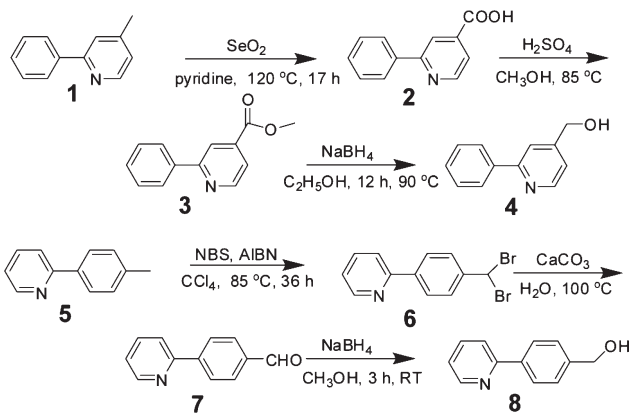

Scheme 2 Synthetic route to phenylpyridine derivatives.

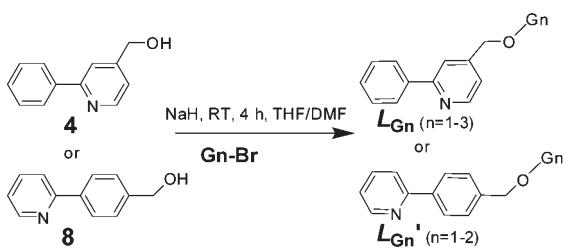

Scheme 3 Synthetic route to dendritic ligands.

The common synthetic route for the cationic iridium complexes involves two steps as illustrated in Scheme 4. The chloro-bridged cyclometalated Ir(III) dimers, (*C^N*)$_2$Ir(μ-Cl)$_2$Ir(*C^N*)$_2$, were synthesized by heating iridium chloride trihydrate ($IrCl_3 \cdot 3H_2O$) with

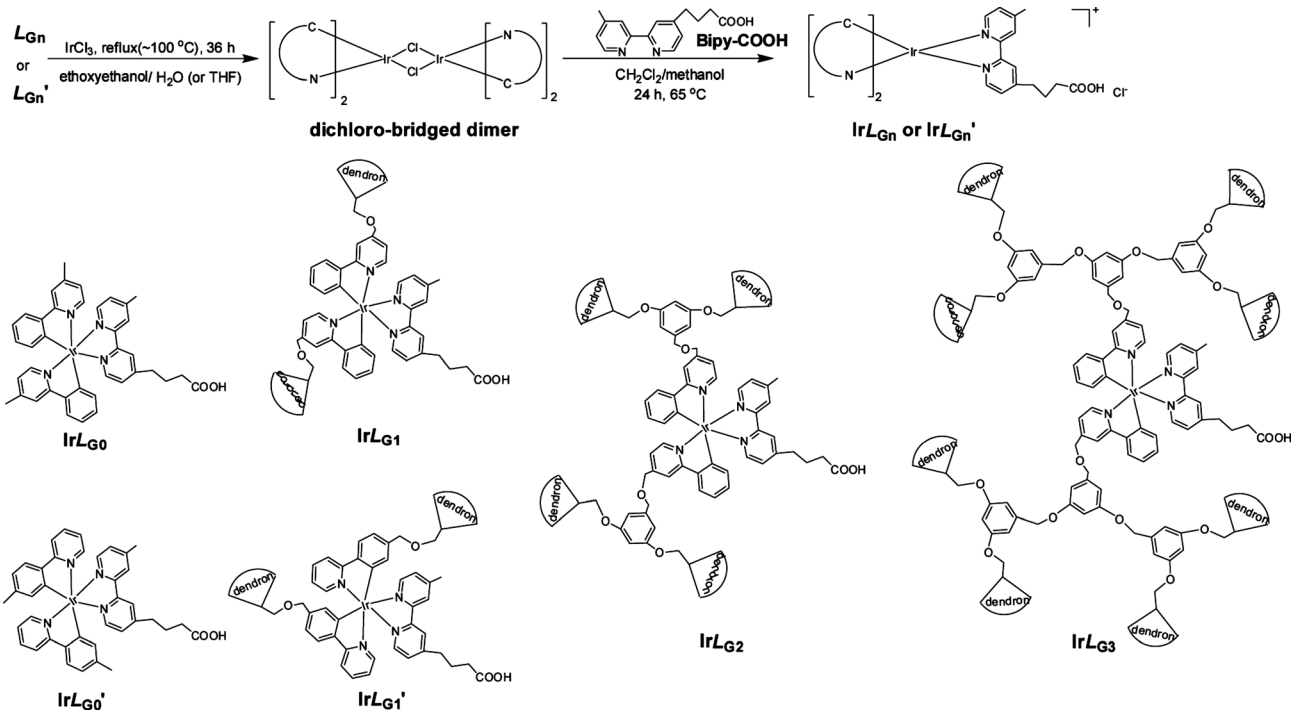

Scheme 4 Synthetic route to dendritic Ir(III) complexes $\mathbf{Ir}\boldsymbol{L}_{Gn}$ and $\mathbf{Ir}\boldsymbol{L}_{Gn}'$.

an excess of the dendritic *C^N* ligands in a mixture of 2-ethoxyethanol/water (3 : 1, v/v) according to the literature.[53] Then the cationic Ir(III) complexes were prepared by refluxing the as-prepared dichloro-bridged dimers and the ancillary bidentate *N^N* ligand, bipy-COOH, in CH_2Cl_2/methanol solution overnight. The introduction of the carboxyl functionalized ancillary ligand makes the Ir(III) complexes bioconjugatable, providing opportunities to be utilized as luminescent probes for bioanalysis or imaging.

When using dendritic ligands, $\boldsymbol{L}_{Gn}$, the yield of the final complexes decreased with the increase of the dendrimer. The first- to third-generation of Ir(III)-cored dendrimers ($\mathbf{Ir}\boldsymbol{L}_{G1}$–$\mathbf{Ir}\boldsymbol{L}_{G3}$) were obtained with yields of 71%, 40%, and 20%, respectively. For the dimerization, because the solubility of $\boldsymbol{L}_{Gn}$ and $\boldsymbol{L}_{Gn}'$ becomes smaller with the increase of the generation number (n), certain amounts of THF were added to the reaction mixtures.

The difference between $\boldsymbol{L}_{Gn}$ and $\boldsymbol{L}_{Gn}'$ lies in the position at which the dendritic scaffolds are rooted. Such a steric difference seems to have a fundamental impact on the reactivity of the $\boldsymbol{L}_{Gn}'$ during the dimerization process. For the $\boldsymbol{L}_{Gn}'$ series, only $\boldsymbol{L}_{G1}'$ could finally form the metal complex $\mathbf{Ir}\boldsymbol{L}_{G1}'$, while $\boldsymbol{L}_{G2}'$ failed to form the dichloro-bridged cyclometalated Ir(III) dimer. Comparing the *meta* position of the carbon atom that forms the C–Ir bond in the phenyl ring of $\boldsymbol{L}_{G2}'$ with the *para* position of the nitrogen atom of $\boldsymbol{L}_{G2}$, the former has a greater steric hindrance, which most likely prevents the formation of the Ir(III) complex dimer. Such a steric effect and the challenge to the synthesis had been envisaged when starting this work. Fortunately, by switching the *C^N* ligands from $\boldsymbol{L}_{Gn}'$ to $\boldsymbol{L}_{Gn}$, we successfully prepared the target compounds with designed functionalities and were able to conduct further characterization.

Among these metal complexes, $\mathbf{Ir}\boldsymbol{L}_{G0}$ and $\mathbf{Ir}\boldsymbol{L}_{G0}'$ are readily soluble in common polar solvents, such as acetonitrile, methanol and ethanol, and non-polar solvents, such as CH_2Cl_2, chloroform and THF, as well. However, $\mathbf{Ir}\boldsymbol{L}_{G1}$, $\mathbf{Ir}\boldsymbol{L}_{G2}$, and $\mathbf{Ir}\boldsymbol{L}_{G3}$ are soluble only in solvents such as CH_2Cl_2, chloroform and THF.

The compounds synthesized in this work were structurally verified with ^1H and ^{13}C NMR spectroscopies and MALDI-TOF mass spectra (see Fig. S16, S18, S20 and S22, ESI†).

As shown in Fig. 1, the ^1H NMR spectra of the dendrimers become very complicated with the growth of dendrimer generation. However, the chemical shifts at 1.8–3.0 ppm, assigned to the aliphatic proton of the bipy-COOH ligand, are very

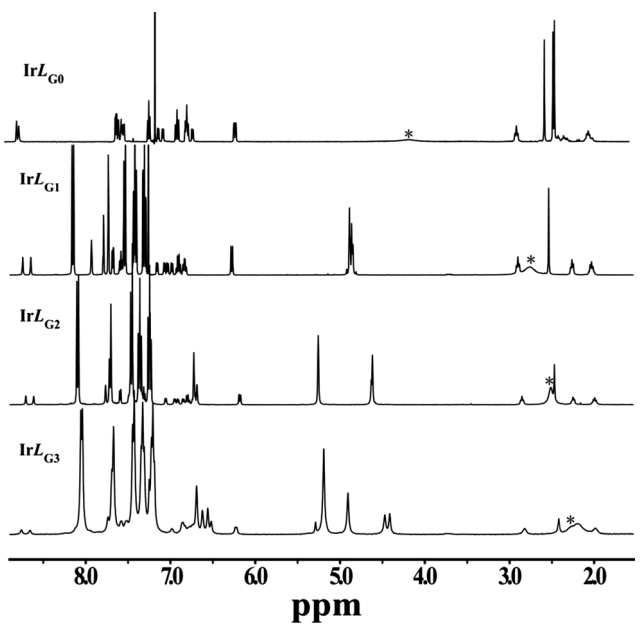

Fig. 1 The ^1H NMR spectra of $\mathbf{Ir}\boldsymbol{L}_{Gn}$ (n = 0–3) in $CDCl_3$ (* denotes signals arising from the active proton.).

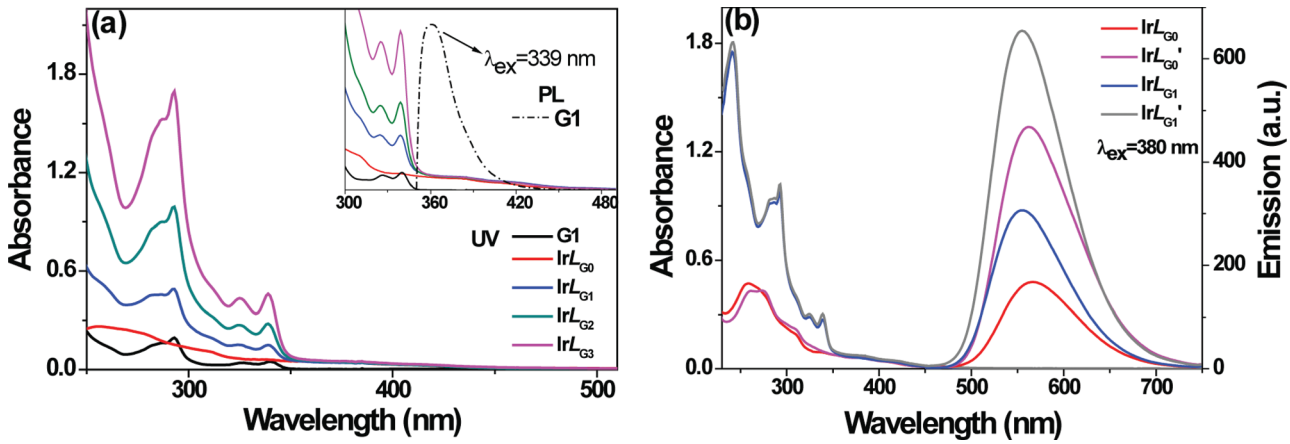

Fig. 2 (a) UV/Vis spectra of Ir(III) complex-cored dendrimers $\mathbf{IrL_{Gn}}$ (n = 0–3) in CH_2Cl_2 solutions (5 μM) at 298 K. The inset shows the fine absorption details in the range from 300 nm to 480 nm and the emission spectrum (dashed line) of 5-methyl-*N*,*N*′-dicarbazolyl-1,3-benzene (**G1**); (b) A comparison between the absorption and the emission spectra of $\mathbf{IrL_{G0}}$–$\mathbf{IrL_{G0}'}$ and $\mathbf{IrL_{G1}}$–$\mathbf{IrL_{G1}'}$.

characteristic and indicative of the proper coordination of the *N*^*N* ligand with the Ir(III) atom. The integration of the aliphatic protons from the bipy-COOH ligand ($\mathbf{IrL_{G1}}$, $\mathbf{IrL_{G2}}$, and $\mathbf{IrL_{G3}}$) and from the additional methyl groups of phenylpyridine (only for $\mathbf{IrL_{G0}}$) match well with the integration of the proton signals within the aromatic region. The signals of the methylene protons of the benzyl ether structure located between 4–5.5 ppm provide further evidence for the structural confirmation. For instance, two sets of overlapped signals at 4.8 ppm were observed for complex $\mathbf{IrL_{G1}}$, which was assigned to the only two kinds of ether methylene. On the other hand, consistent with its four ether methylene groups, four sets of signals with an integral ratio of 16 : 8 : 4 : 4 in the range from 4.4 to 5.2 ppm were observed for $\mathbf{IrL_{G3}}$.

The absorption spectra, which will be discussed in detail in the following section, provide extra evidence to support the structures of $\mathbf{IrL_{G1}}$–$\mathbf{IrL_{G3}}$, which have 4, 8 and 16 peripheral carbazolyl groups, respectively. Corresponding to the linear increase of the number of carbazolyl groups, we observed the same linear increase in the relative absorbance (at *e.g.*, 339 nm) of the carbazolyl groups (Fig. 2).

Photophysical and electrochemical properties

As a common solvent, CH_2Cl_2 was chosen as the solvent for the photophysical characterization of the dendritic metal complexes. The UV/Vis absorption spectra of $\mathbf{IrL_{Gn}}$ (n = 0–3) and $\mathbf{IrL_{Gn}'}$ (n = 0–1) in CH_2Cl_2 solutions are depicted in Fig. 2.

The complex $\mathbf{IrL_{G0}}$ presents very broad and overlapped absorption bands, which are assigned to the typical intra-ligand charge transfer (ILCT) transition (<350 nm) and the metal-to-ligand charge transfer (MLCT) transition (>350 nm) of cyclometalated Ir(III) complexes. The Ir(III) complex-cored dendrimers $\mathbf{IrL_{Gn}}$ (n = 1–3) exhibit very similar absorption spectra in CH_2Cl_2 at room temperature. Each of them has clear absorption maxima at 292, 325 and 339 nm. Compared with the absorption spectrum of **G1**, the absorption bands below 350 nm are obviously originating from the spin allowed π–π* transitions of carbazolyl groups and overlapped with the ILCT band of the Ir(III) complex core. In the lower energy region from 350 to 500 nm, a featureless, much weaker absorption band also appeared due to the MLCT transitions of the Ir(III) complexes. With the increase of the number of carbazolyl groups from the $\mathbf{IrL_{G1}}$ dendrimer to the $\mathbf{IrL_{G3}}$ dendrimer, the molar extinction coefficient of the π–π* transitions of carbazolyl groups increased gradually, but the MLCT bands of $\mathbf{IrL_{Gn}}$ (n = 0–3) remained almost unchanged. From the comparison of the absorption spectra between $\mathbf{IrL_{G0}}$ and $\mathbf{IrL_{G0}'}$, and between $\mathbf{IrL_{G1}}$ and $\mathbf{IrL_{G1}'}$, we found that introducing the dendritic branches bearing peripheral carbazolyl groups at the phenyl ring and at the pyridinyl ring of the cyclometalating ppy ligand has almost the same effect on the absorption of the final dendritic cyclometalated Ir(III) complexes (Fig. 3). The results are consistent with other previously reported metal complex systems with dendritic attachments.[54–56]

An emission spectrum of carbazolyl groups in **G1** is also demonstrated in the inset of Fig. 2(a). With a maximum at 360 nm, the emission spans from about 350 to 450 nm; this range perfectly matches the MLCT absorption band of $\mathbf{IrL_{G0}}$ and the dendritic Ir(III) complexes $\mathbf{IrL_{Gn}}$ (n = 1–3), suggesting an efficient energy transfer that could likely occur from the carbazolyl groups to the Ir(III) complex core.

The photoluminescence (PL) emission spectra (Fig. 3(a)) of $\mathbf{IrL_{Gn}}$ (n = 0–3) obtained in degassed CH_2Cl_2 solutions show negligible differences when excited at 380 nm, which falls into the MLCT absorption band of the Ir(III) complexes. The blue shift in the emission maximum from $\mathbf{IrL_{G0}}$ to $\mathbf{IrL_{Gn}}$ (n = 1–3) is only marginally significant. The same blue shift has also been observed from the emission spectrum of $\mathbf{IrL_{G0}'}$ to that of $\mathbf{IrL_{G1}'}$. Similar to the iridium(III) complexes, ruthenium(III) polydiimine complexes show also the blue shift when an ether substitution moiety is attached to the ligand ring.[57]

The relative PL quantum yields (Φ) of the Ir(III) complexes are almost constant with the increase of the generation of carbazolyl dendrons except for $\mathbf{IrL_{G3}}$, which possesses a relatively lower quantum efficiency. It indicates that tethering the benzyl ether dendrons containing carbazolyl termini to the Ir(III) complex core does not noticeably affect the PL properties of the Ir(III) complexes. A similar phenomenon was also observed by Lo *et al.*,[55] Ding *et al.*[58] and Li *et al.*[45]

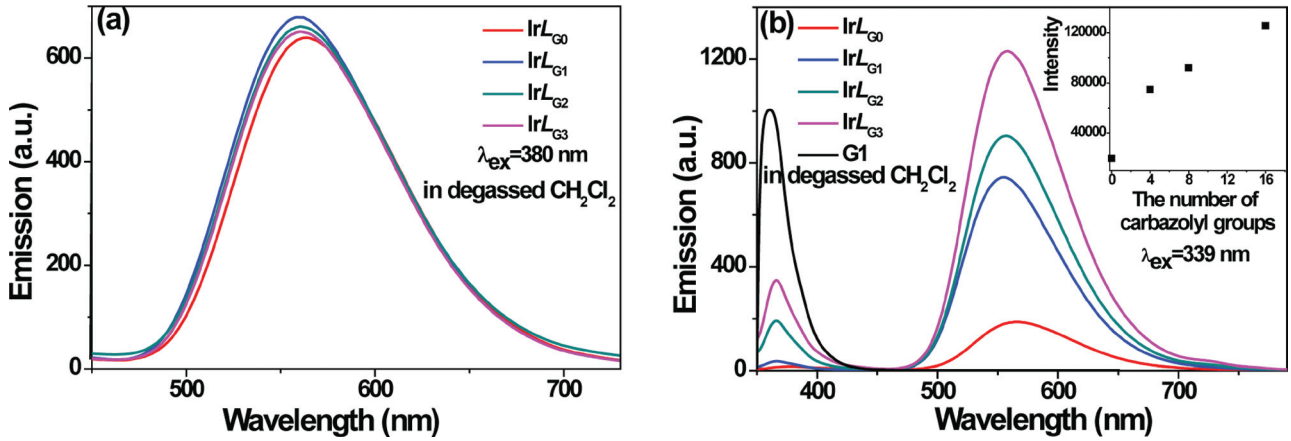

Fig. 3 Emission spectra of a series of Ir(III) complex-cored compounds measured in degassed CH_2Cl_2 solutions (10 μM) when excited by UV light at 380 nm (a) and when excited at 339 nm (b).

However, when the same systems were excited with light at 339 nm, a dramatic change in the emission intensity was observed as demonstrated in Fig. 3(b). By incorporating carbazolyl groups into the Ir(III) complex, we observed a monotonic increase of the emission from $\mathbf{IrL_{G0}}$ to $\mathbf{IrL_{G3}}$. Between the data in Fig. 3(a) and in Fig. 3(b), the distinctive difference lies in the excitation wavelength. As shown in the absorption spectra (Fig. 2), the wavelength of 339 nm corresponds to the first absorption peak of carbazolyl-containing compounds and exciting these compounds with the 339 nm light leads to an emission of 360 nm from carbazolyl groups. The remarkable emission enhancement of the $\mathbf{IrL_{Gn}}$ with the increase of the dendrimer generation *n*, and thus the number of carbazolyl groups, is indicative of the FRET effect. The effect of the excitation wavelength is also demonstrated in the excitation spectra (Fig. S3, ESI†), from which we can see the excitation in the window of about 315–340 nm (corresponding to the carbazole absorption) becomes progressively more efficient with the increase of the dendrimer generation. This is another clear indication of the FRET effect.

In Fig. 3(b), the 360 nm emissions of the carbazolyl groups in $\mathbf{IrL_{Gn}}$ are also depicted. $\mathbf{IrL_{G3}}$, which has sixteen carbazolyl groups, showed a much lower emission than a single dendron (**G1**), which contains only two carbazolyl groups, suggesting an efficient energy transfer. The existence of this peak suggests that not all the emissive energy was transferred to Ir(III) luminophores.

Carbazole has been chosen as an energy donor to Ir(III) complexes because of their higher singlet and triplet emission energies and the perfect match to the MLCT absorption;[45–48] our work further proves that the energy transfer from carbazolyl groups to the Ir(III) complexes is efficient. Increasing the number of carbazolyl groups at both the *C^N* ligands can be a plausible strategy for achieving a meaningful emission enhancement, but complete energy transfer can hardly be achieved as evidenced by the residual emission at 360 nm (in Fig. 3(b)).

A quantitative description of the emission intensity *versus* the number of carbazole units from the light-harvesting antenna demonstrates that the luminescent intensity was enhanced by more than 7 times when comparing $\mathbf{IrL_{G3}}$ with $\mathbf{IrL_{G0}}$. However, due to synthetic difficulties, higher generation dendrimers bearing larger numbers of carbazolyl groups were not available in this work, and thus the function of the emission intensity *vs.* the number of carbazolyl groups or *vs.* the number of dendrimer generation is hardly available based on the limited data from only $\mathbf{IrL_{G0}}$, $\mathbf{IrL_{G1}}$, $\mathbf{IrL_{G2}}$ and $\mathbf{IrL_{G3}}$.

An ideal FRET should fulfill several key requirements: the coexistence of donor–acceptor, the spectral match, and a suitable distance between the donor and acceptor. According to Förster's equation, the FRET rate constant correlates with r^{-6} (in the range of 10–100 Å) where *r* represents the distance between the donor and acceptor.[59] According to a simple structural simulation,[60] we have estimated the donor–acceptor distances to be 9.17 Å, 13.38 Å and 27.4 Å in $\mathbf{IrL_{G1}}$, $\mathbf{IrL_{G2}}$ and $\mathbf{IrL_{G3}}$, respectively. We assumed that the elongation of the donor–acceptor distance in higher generations of dendritic complexes, such as $\mathbf{IrL_{G3}}$, could diminish the energy transfer efficiency and result in a smaller PL enhancement effect. Unfortunately, the limited number of data points could not enable a conclusion to be drawn.

We have also performed electrochemical characterization by cyclic voltammetry to acquire the redox properties of these complexes. The cyclic voltammograms of $\mathbf{IrL_{Gn}}$ (n = 0–3) are displayed in Fig. S4, ESI.† All these complexes displayed a one-electron reduction wave between −1.94 V and −1.84 V with a good reversibility. Based on the studies on some 2,2′-bipyridine metal complexes, for example, $Ru(bipy)_3^{2+}$[61] and $(C^N)_2Ir(dtb\text{-}bipy)$,[62] the reduction wave is associated with a ligand (bipy-COOH) centered process. But, except for $\mathbf{IrL_{G0}}$, the carbazolyl functionalized $\mathbf{IrL_{Gn}}$ (n = 1–3) did not show well-defined oxidation waves with an observable reversibility. For this reason, the oxidation potentials for these complexes are hard to determine. The available electrochemical data are summarized in Table 1.

Oxygen quenching/shielding

The photophysical studies discussed above were experimentally based on the employment of fully deaerated solutions. In air saturated CH_2Cl_2 solutions, under excitation at 380 nm, which does not cause a FRET effect, we have found a large variation of the emission intensities of $\mathbf{IrL_{Gn}}$ (n = 1–3) as shown in Fig. 4. The emission spectra, which almost overlap with each other in the deaerated CH_2Cl_2 solutions (Fig. 2(a)), are largely separated in the air saturated solutions (Fig. 4). We believe that oxygen in

Table 1 Photophysical and electrochemical properties of dendritic Ir(III) complexes $\mathbf{IrL_{Gn}}$ (n = 0–3)

Complex	Absorbance	Emission[a]		Redox Potentials[b]	
	λ (ε, $\times 10^4$ $M^{-1}cm^{-1}$)	λ_{max} (nm)	Φ	$E_{1/2}^{Ox}$(V)	$E_{1/2}^{red}$(V)
$\mathbf{IrL_{G0}}$	255(2.6)	566	0.31	0.75[d]	−1.94[d]
$\mathbf{IrL_{G1}}$	293(4.9), 324(1.5), 339(1.5)	555	0.30	0.80[c]	−1.84[d]
$\mathbf{IrL_{G2}}$	293(9.9), 325(2.7), 339(2.8)	557	0.30	0.72[c]	−1.93[d]
$\mathbf{IrL_{G3}}$	293(17.0), 324(4.3), 339(4.6)	558	0.24	0.76[c]	−1.87[d]

[a] Measured in degassed CH_2Cl_2 solution and calculated by using $Ir(ppy)_3$ (Φ = 0.90 in dichloroethane, a very high quantum efficiency of $Ir(ppy)_3$ reported by Adachi *et al.* recently[32]) as standard reference; [b] Measured in DMF with $\mathbf{IrL_{Gn}}$ concentration of 0.4 mM; Potential values referenced to Fc/Fc^+ [c] irreversible wave; [d] reversible wave.

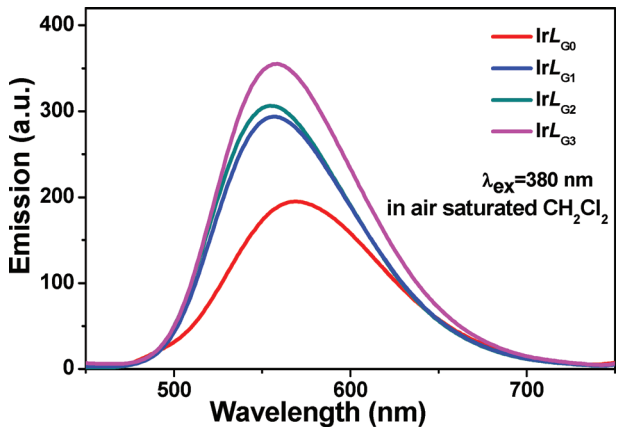

Fig. 4 Emission spectra of a series of Ir(III) complex-cored dendrimers measured in air saturated CH_2Cl_2 solutions (10 μM) when excited by UV light at 380 nm.

the air and the shielding effect of the dendritic scaffolds play roles in the observed emission features.

It is known that the cyclometalated Ir(III) complexes are sensitive to molecular oxygen and their phosphorescent emission can be readily quenched.[63,64] The mechanism of this quenching effect involves the long-lived triplet excited state of Ir(III) complexes undergoing efficient energy transfer to the triplet ground state of molecular oxygen and results in nonradiative relaxation of the Ir(III) luminophore and the generation of singlet oxygen. Actually, Fig. 4 not only shows the separation of the PL from different metal complexes that have almost the same emission properties in deaerated solvent, but discloses a reduction of all the PL intensities. It is interesting to note that $\mathbf{IrL_{G0}}$ underwent the biggest change in PL intensity while $\mathbf{IrL_{G3}}$ was least influenced by molecular oxygen. A plausible assumption is that the benzyl ether dendrimers with carbazolyl termini act as an outer shield of oxygen and protect the excited state of the Ir(III) complex core from being quenched by oxygen.

The oxygen sensitivity of luminophores can be utilized to develop oxygen sensors for various applications including those in bio-imaging[65] and environmental analysis.[66] It is, however, a drawback when using Ir(III) complexes for some other purposes in which the emission intensity is correlated to a physical or chemical quantity of interest.

The shielding effect of dendritic aromatic branches surrounding a ruthenium complex core[67,68] has been reported. There is little doubt that the different effects of oxygen on the PL of $\mathbf{IrL_{Gn}}$ (n = 1–3) is a result of different shielding degrees, which is related to the complexity of dendritic structure surrounding the Ir(III) complex core. A quantitative description of the oxygen quenching or shielding was conducted based on the studies of the luminophores exposed to the oxygen at different levels.

From the oxygen-free solutions to the oxygen-saturated solutions, the four $\mathbf{IrL_{Gn}}$ (n = 0–3) exhibited a PL intensity decrease with factors of 12.04, 11.65, 9.89 and 9.00-fold, respectively. Detailed in Fig. 5 are the PL emission spectra of $\mathbf{IrL_{G3}}$ exposed to five different oxygen levels (other complexes showed similar trends and are reported in Fig. S5, ESI†).

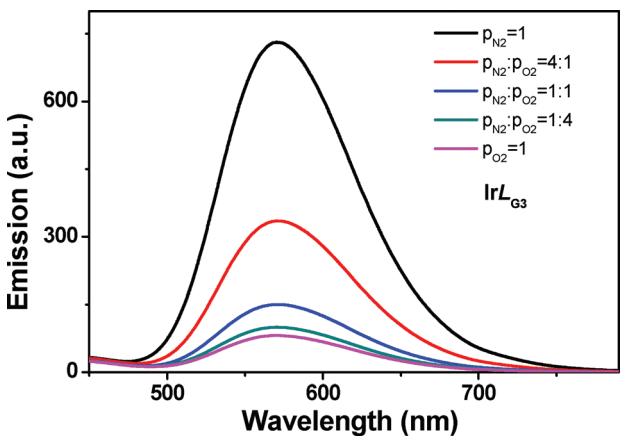

Fig. 5 Emission spectra of 10 μM $\mathbf{IrL_{G3}}$ in DMF recorded under different oxygen partial pressures (p_{O_2}) at room temperature. Excitation wavelength 380 nm, at which no FRET could possibly take place.

A linear correlation between I_0/I and p_{O_2} was plotted in Fig. 6 according to the Stern–Volmer equation $I_0/I = 1+K_{SV}p_{O_2}$, from which the quenching constants, K_{SV}, were deducted. They are 10.60, 9.81, 8.48 and 7.30 atm^{-1} for $\mathbf{IrL_{Gn}}$ (n = 0–3), respectively. A gradual lowering of K_{SV} indicates reduced sensitivity of the luminophores to molecular oxygen as the dendritic scaffold becomes larger.[20,69]

Conclusions

A series of bioconjugatable, cationic cyclometalated Ir(III) complexes containing a dendritic carbazole energy donor on the cyclometalating *C^N* ligands was successfully synthesized and thoroughly characterized. Photophysical studies revealed that the cationic Ir(III) complex core and the carbazolyl terminated

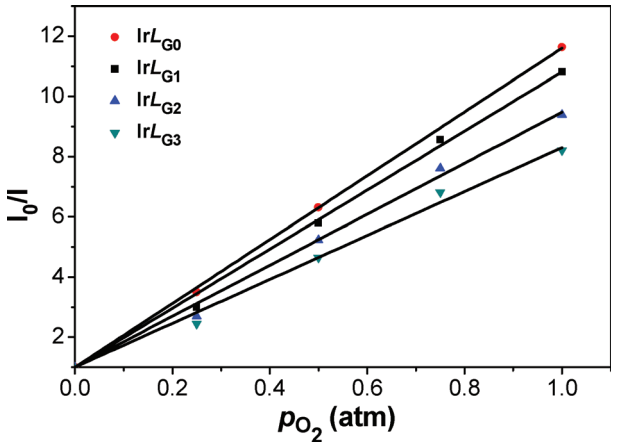

Fig. 6 Stern–Volmer plots for the oxygen quenching of 10 μM of **IrL_{Gn}** (n = 0–3) in DMF at room temperature.

dendrimers constructed an efficient donor–acceptor energy transfer system, in which the dendritic carbazole moiety could efficiently transfer energy *via* a FRET pathway leading to a remarkable PL enhancement of the Ir(III) complexes. In addition to the FRET effect, the dendritic structure, including the branch and the peripheral carbazolyl groups, form a shield that prevents the luminophore core from being quenched by molecular oxygen under the photo excitation. The dual functions, *i.e.* energy donor and oxygen shield, of the designed structures suggest further exploitation of this system, in particular because of the bioconjugatability, for applications in biological and biochemical areas.

Experimental section

Materials

All solvents were of analytical reagent grade and purified according to standard procedures. *Trans*-1,2-diaminocyclohexane was purchased from Aldrich. Carbazole, *N*-bromosuccinimide, $IrCl_3 \cdot 3H_2O$, 2-*p*-tolylpyridine (**5**), 1,3-dibromo-5-methylbenzene and 3,5-dihydroxybenzyl alcohol were commercial products and used without further purification. The carbazolyl-type dendritic benzyl bromides **G1-Br** and **G2-Br** and **G3-Br** were prepared according to the procedures developed by Kwon.[46] 4-methyl-2-phenylpyridine (**1**) and bipy-COOH (4-(4′-methyl-2,2′-bipyridin-4-yl)butanoic acid) were obtained from SunaTech Inc. (>99%) and used without further purification.

Measurements

^1H and ^{13}C NMR spectra were acquired on a VARIAN 400 MHz magnetic resonance spectrometer. The UV-Vis absorption spectra and emission spectra were obtained on a Perkin Elmer Lambda 25 UV-Vis spectrophotometer and a HITACHI F-4600 spectrofluorophotometer, respectively. Mass analysis was carried out on an Agilent TOF spectrometer (ESI-MS). Matrix assisted laser desorption/ionization time-of-flight mass spectroscopic (MALDI-TOF-MS) data were obtained by a Bruker APEX-II spectrometer at an acceleration voltage of 19 000 V with α-cyano-4-hydroxycinnamic acid as the matrix. Relative photoluminescence quantum efficiencies of the synthesized compounds were measured in degassed CH_2Cl_2 solutions by using Ir(ppy)$_3$ (Φ = 0.90 in dichloroethane solution[32]) as a reference compound at room temperature. Cyclic voltammetry (CV) measurements were performed using a PARSTAT 2263 Advanced Electrochemical System with PowerSUITE software. Each sample was prepared by dissolving 2 μmol of Ir(III) complex in 5 mL anhydrous DMF with 0.1 M tetrabutylammonium hexafluorophosphate as the electrolyte and all measurements were conducted at room temperature. A platinum disk (1 mm in diameter) sealed in a PTFE rod was used as the working electrode. A piece of platinum wire and a piece of silver wire were used as the counter electrode and the quasi-reference electrode, respectively. The potentials were calibrated with the ferrocene/ferrocenium Fc/Fc$^+$ redox couple ($E_{1/2}$ = 0.35 V *vs.* Ag/AgCl). The potential scan rate in all the experiments was kept at 100 mV s^{-1}.

Oxygen quenching test

All PL measurements were conducted in anhydrous DMF solution with 10 μM of Ir(III) complexes at room temperature. The volume concentration of oxygen in the gas mixture was controlled by adjusting the flow rates of the oxygen and the nitrogen streams flowing into a mixing chamber. The Ir(III) complex solutions were purged with the mixed gas stream from the mixing chamber for 30 min prior to the PL measurement. The oxygen quenching effects were evaluated by the Stern–Volmer equation: $I_0/I = 1+K_{SV}p_{O_2}$, where I_0 and I are the luminescence intensities for the oxygen-free solutions and the solutions flushed by gas flow with different oxygen partial pressure (p_{O_2}), respectively. The Stern–Volmer quenching constant, K_{SV}, was obtained from a linear plot of (I_0/I) *versus* p_{O_2}.

Synthesis and characterization

2-Phenyl-4-carboxypyridine (2). This compound was prepared according to the literature procedure (Scheme 2).[70] 4-methyl-2-phenylpyridine (**1**) (2.1 g, 12.4 mmol) and SeO_2 (10.8 g, 97.3 mmol) were refluxed in pyridine (100 mL) for 24 h under an argon atmosphere. After the reaction, the mixture was then filtered through Celite while hot. The solid was obtained after washing with water (60 mL). The resulting light brown solid was suspended in a mixture of methanol (70 mL) and water (50 mL) and made basic by addition of an aqueous NaOH solution to pH 9–10. After filtration of insoluble materials, the filtrate was then acidified with concentrated HCl to pH 2–3. The organic solution of methanol was evaporated and the formed precipitate was filtered, washed with water and finally dried *in vacuo* to afford 2.0 g (yield: 81%) of the titled compound as a slightly brown solid. ^1H NMR (δ (ppm), DMSO-d_6, 400 MHz): 13.75 (s, 1H), 8.87 (d, J = 5.2 Hz, 1H), 8.29 (s, 1H), 8.14–8.11 (m, 2H), 7.79 (d, J = 5.2 Hz, 1H), 7.55–7.46 (m, 3H).

Methyl 2-phenyl-4-carboxypyridine (3). This compound was prepared according to the literature procedure (Scheme 2).[67] 2-phenyl-4-carboxypyridine (**2**) (2.0 g, 10.0 mmol) was refluxed in methanol (50 mL) and H_2SO_4 (3 mL) for 12 h. After the reaction, the organic solvent was evaporated and water (100 mL) was added. The mixture was neutralized with saturated $NaHCO_3$ solution to pH ~7. The resulting solution was extracted twice with CH_2Cl_2 (2 × 100 mL) and dried over anhydrous $MgSO_4$.

The crude compound was purified by silica gel column chromatography eluting with CH_2Cl_2 to give **3** (2.1 g, 99%) as a colorless oil. ^{1}H NMR (δ (ppm), $CDCl_3$, 400 MHz): 8.84 (d, J = 5.2 Hz, 1H), 8.30 (s, 1H), 8.07–8.04 (m, 2H), 7.77 (d, J = 5.2 Hz, 1H), 7.52–7.42 (m, 3H), 3.99 (s, 3H).

2-Phenylpyridyl-4-methanol (4). A suspension of compound **3** (0.9 g, 4.7 mmol) and sodium borohydride (1.0 g, 26.4 mmol) in 50 mL of ethanol was refluxed for 12 h. After reaction, the mixture was cooled to room temperature, and then 80 mL of a saturated ammonium chloride aqueous solution was added to decompose the excess sodium borohydride. Most of the ethanol was removed by rotary evaporation. The resulting solution was extracted three times with ethyl acetate (3 × 50 mL) and dried over anhydrous sodium sulfate. After the solvent was removed *in vacuo*, the crude product was subsequently purified by silica gel column chromatography eluting with CH_2Cl_2/EtOAc (1 : 1, v/v) to give **4** (0.7 g, 80%) as a colorless oil. ^{1}H NMR (δ (ppm), $CDCl_3$, 400 MHz): 8.62 (d, J = 5.2 Hz, 1H), 7.99–7.96 (m, 2H), 7.71 (s, 1H), 7.49–7.39 (m, 3H), 7.20 (d, J = 5.2 Hz, 1H), 4.78 (s, 2H).

2-(4-(Dibromomethyl)phenyl)pyridine (6). To a mixture of 2-*p*-tolylpyridine (**5**) (5.0 g, 29.5 mmol) and *N*-bromosuccinimide (NBS) (11.6 g, 65.0 mmol) in CCl_4 (100 mL) was added azobisisobutyronitrile (AIBN) (80.0 mg, 4.8 mmol). After refluxing for 36 h, the reaction mixture was cooled to room temperature and filtered to remove precipitates. The filtrate was evaporated and purified by silica gel column chromatography eluting with CH_2Cl_2/hexane/EtOAc (10 : 30 : 1, v/v/v) to give **6** (7.3 g, 75%) as a white powder. ^{1}H NMR (δ (ppm), $CDCl_3$, 400 MHz): 8.71–8.70 (m, 1H), 8.01 (d, J = 8.4 Hz, 2H), 7.79–7.72 (m, 2H), 7.68 (d, J = 8.4 Hz, 2H), 7.28–7.25 (m, 1H), 6.71(s, 1H).

4-(Pyridin-2-yl)benzaldehyde (7). Compound **6** (4.5 g, 13.8 mmol) was transferred to a 250 mL flask and mixed thoroughly with 20.0 g (0.2 mol) of powdered calcium carbonate. About 100 mL of water was added and the mixture was heated cautiously and then refluxed for 15 h to enable efficient hydrolysis. After subsequent cooling and filtration, the filtrate was extracted with CH_2Cl_2 and dried over anhydrous Na_2SO_4. After evaporation *in vacuo*, a crude product was obtained and purified by silica gel column chromatography eluting with CH_2Cl_2 to give pure aldehyde **7** (2.0 g, 80%). ^{1}H NMR (δ (ppm), $CDCl_3$, 400 MHz): 10.09 (s, 1H), 8.75–8.74 (m, 1H), 8.19–8.17 (m, 2H), 8.00–7.98 (m, 2H), 7.82–7.80 (m, 2H), 7.34–7.29 (m, 1H).

(4-(Pyridin-2-yl)phenyl)methanol (8). Sodium borohydride (0.4 mg, 10.6 mmol) was added to a solution of aldehyde **7** (2.0 g, 10.9 mmol) in 80 mL of methanol. The mixture was stirred for 30 min in an ice-bath and for 2.5 h at room temperature. After reaction, 40 mL of saturated ammonium chloride aqueous solution was added to decompose the excess sodium borohydride. Most of the methanol was removed by rotary evaporation. The resulting solution was extracted with CH_2Cl_2 and dried over anhydrous sodium sulfate. After the solvent was removed *in vacuo*, the target product was obtained (1.9 g, 92%). ^{1}H NMR (δ (ppm), $CDCl_3$, 400 MHz): 8.69–8.67 (m, 1H), 7.97–7.95 (m, 2H), 7.78–7.70 (m, 2H), 7.47–7.43 (m, 2H), 7.25–7.22 (m, 1H), 4.75 (s, 2H).

General synthetic route for the *C^N* ligands bearing carbazolyl at the dendritic peripheries L_{Gn} (n = 1–3) and L_{Gn}' (n = 1–2)

The cyclometalating ligands have the general structures shown in Scheme 3. L_{Gn} (n = 1–3) series have their dendritic moieties at the pyridine ring and the L_{Gn}' (n = 1–2) series at the phenyl ring. Each series shares the same starting materials, *i.e.*, (2-phenylpyridin-4-yl)methanol **4** or (4-(pyridin-2-yl)phenyl)methanol **8** respectively.

For n = 1, the corresponding phenylpyridine derivative (**4** or **8**) (1.0 equiv.) was dissolved in anhydrous THF. After NaH (2 equiv.) was added, the reaction mixture was stirred for 30 min in an ice-bath. Then a solution of **G1-Br** (1.5 equiv.) in anhydrous THF was added. After stirring for 4 h under an argon atmosphere, the reaction was quenched by slowly pouring the mixture into water. After most of the THF was evaporated, the water phase was extracted with CH_2Cl_2. The organic layer was dried over anhydrous sodium sulfate and evaporated *in vacuo*. The crude product was obtained and purified by silica gel column chromatography eluting with CH_2Cl_2. Yield: 67–78%.

For n = 2 and 3, because of the poor solubility of **G2-Br** and **G3-Br** in THF, DMF was used as the reaction solvent. After the reaction was complete, it was terminated with water. The light yellow precipitate was filtered over Celite and purified by silica gel chromatography eluting with CH_2Cl_2/hexane (from 3 : 1 to 1 : 3, v/v). Yield: 75–85%.

L_{G1}: (Yield: 78%). ^{1}H NMR (δ (ppm), $CDCl_3$, 400 MHz): 8.67 (d, J = 4.8 Hz, 1H), 8.15 (d, J = 7.6 Hz, 4H), 7.97–7.95 (m, 2H), 7.79–7.74 (m, 4H), 7.54 (d, J = 8.0 Hz, 4H), 7.44–7.40 (m, 7H), 7.33–7.25 (m, 5H), 4.85 (s, 2H), 4.79 (s, 2H). ^{13}C NMR (δ (ppm), $CDCl_3$, 100.65 MHz): 157.71, 149.64, 147.88, 141.77, 140.48, 139.55, 138.93, 129.11, 128.76, 126.97, 126.17, 124.41, 124.36, 123.63, 120.47, 120.41, 120.32, 118.67, 109.63, 71.92, 71.28.

L_{G2}: (Yield: 82%). ^{1}H NMR (δ (ppm), $CDCl_3$, 400 MHz): 8.64–8.63 (m, 1H), 8.12 (d, J = 7.6 Hz, 8H), 7.89 (d, J = 8.0 Hz, 2H), 7.76 (s, 6H), 7.69–7.65 (m, 1H), 7.58 (d, J = 8.0 Hz, 1H), 7.50 (d, J = 8.0 Hz, 8H), 7.42–7.38 (m, 10H), 7.30–7.25 (m, 8H), 7.19–7.16 (m, 1H), 6.74 (d, J = 2.0 Hz, 2H), 6.68 (t, J = 2.0 Hz, 1H), 5.30 (s, 4H), 4.60 (s, 2H), 4.56 (s, 2H). ^{13}C NMR (δ (ppm), $CDCl_3$, 100.65 MHz): 159.58, 156.97, 149,58, 141.31, 140.81, 140.40, 139.53, 138.81, 138.74, 138.67, 128.09, 126.91, 126.46, 124.29, 124.18, 123.59, 122.05, 120.42, 120.37, 109.66, 107.00, 101.79, 71.87, 71.78, 69.07.

L_{G3}: (Yield: 85%). ^{1}H NMR (δ (ppm), $CDCl_3$, 400 MHz): 8.54 (d, J = 5.2 Hz, 1H), 8.07 (d, J = 7.6 Hz, 15H), 7.92–7.9 (m, 2H), 7.71–7.69 (m, 12H),7.58 (s, 1H), 7.45 (d, J = 8.0 Hz, 15H), 7.37–7.33 (m, 19H), 7.25–7.21 (m, 18H), 7.05 (d, J = 4.4 Hz, 1H), 6.71 (d, J = 2.0 Hz, 4H), 6.63 (t, J = 2.0 Hz, 2H), 6.55 (d, J = 2.0 Hz, 2H), 6.51 (d, J = 2.0 Hz, 1H), 5.22 (s, 8H), 4.93 (s, 4H), 4.42 (s, 2H), 4.39 (s, 2H). MALDI-TOF-MS: m/z 2233.0 $[M-Cl]^+$, 2256.0 $[M + Na]^+$.

L_{G1}': (Yield: 67%). ^{1}H NMR (δ (ppm), $CDCl_3$, 400 MHz): 8.70–8.68 (m, 1H), 8.15 (d, J = 7.6 Hz, 4H), 8.00–7.98 (m, 2H), 7.77–7.70 (m, 5H), 7.56–7.51 (m, 6H), 7.46–7.42 (m, 4H), 7.33–7.29 (m, 4H), 7.25–7.21 (m, 1H), 4.78 (d, J = 6.0 Hz, 4H). ^{13}C NMR (δ (ppm), $CDCl_3$, 100.65 MHz): 156.98, 149.62, 142.37, 140.47, 139.33, 138.97, 138.48, 136.73, 128.13, 127.05, 126.12, 124.53, 124.11, 123.54, 122.12, 120.47, 120.40, 120.29, 109.70, 72.52, 71.22.

L_{G2}': (Yield: 75%). ^{1}H NMR (δ (ppm), $CDCl_3$, 400 MHz): 8.67 (d, J = 4.0 Hz, 1H), 8.13 (d, J = 7.6 Hz, 7H), 7.76 (s, 6H), 7.61 (d, J = 8.4 Hz, 1H), 7.51–7.49 (m, 8H), 7.43–7.30 (m, 10H), 7.30–7.25 (m, 11H), 6.74 (d, J = 2.0 Hz, 2H), 6.68 (t, J = 2.0 Hz, 1H), 5.31 (s, 4H), 4.60 (s, 2H), 4.57 (s, 2H).

General synthetic route for IrL_{Gn} (n = 0–3) and IrL_{Gn}' (n = 0–2)

$IrCl_3 \cdot 3H_2O$ and 2.5 equiv. of cyclometalating ligand (L_{Gn} or L_{Gn}') were added into a mixture of 2-methoxyethanol and water (3 : 1, v/v), and the reaction mixture was refluxed for 36 h to yield the corresponding dichloro-bridged dimer complexes. After cooling to room temperature, the solution was filtered through Celite and the yellow precipitate was washed with water, ether and hexane and dried *in vacuo*. The obtained dimer and 2.2 equiv. of bipy-COOH were added to CH_2Cl_2 (CH_2Cl_2/methanol for IrL_{G0} and IrL_{G0}'), and the reaction mixture was refluxed under an inert atmosphere for 24 h. After cooling to room temperature, the crude product was purified by silica gel column chromatography with CH_2Cl_2/methanol (various ratios based on the mixture properties) eluent to give the pure product. Yield: 84–20%.

IrL_{G0}: (Yield: 84%). ^{1}H NMR (δ (ppm), $CDCl_3$, 400 MHz): 8.85–8.84 (m, 2H), 7.74–7.63 (m, 6H), 7.34–7.32 (m, 2H), 7.23 (d, J = 5.6 Hz, 2H), 7.17 (d, J = 5.6 Hz, 1H), 7.00 (t, J = 7.6 Hz, 2H), 6.90–6.86 (m, 3H), 6.82 (d, J = 6.0 Hz, 1H), 6.32–6.29 (m, 1H), 4.28 (br), 2.94 (t, J = 7.2 Hz, 2H), 2.62 (s, 3H), 2.51 (d, J = 5.6 Hz, 6H), 2.42–2.33 (m, 2H), 2.10–2.04 (m, 2H). ^{13}C NMR (δ (ppm), $CDCl_3$, 100.65 MHz): 177.42, 167.30, 167.04, 156.02, 155.81, 155.42, 151.94, 150.96, 150.88, 149.66, 149.58, 149.23, 148.00, 147.71, 143.67, 143.49, 131.86, 131.76, 130.46, 130.33, 128.49, 128.26, 126.32, 125.98, 124.47, 124.42, 124.35, 124.18, 122.26, 122.19, 120.24, 120.07, 35.65, 34.92, 26.32, 21.50, 21.37, 21.34. TOF-MS (ESI): Calcd. for $[M-Cl]^+$ 785.2468; found, 785.2461.

IrL_{G1}: (Yield: 71%). ^{1}H NMR (δ (ppm), $CDCl_3$, 400 MHz): 8.74 (s, 1H), 8.64 (s, 1H), 8.15 (d, J = 7.6 Hz, 8H), 7.93 (s, 2H), 7.79 (t, J = 2.0 Hz, 2H), 7.73 (d, J = 2.0 Hz, 4H), 7.68 (d, J = 5.6 Hz, 2H), 7.60–7.57 (m, 2H), 7.54 (d, J = 8.0 Hz, 8H), 7.44–7.40 (m, 10H), 7.33–7.29 (m, 8H), 7.16 (d, J = 5.6 Hz, 1H), 7.07 (d, J = 5.6 Hz, 1H), 7.03 (d, J = 6.0 Hz, 1H), 6.98 (d, J = 6.0 Hz, 1H), 6.94–6.88 (m, 2H), 6.86–6.80 (m, 2H), 6.29 (t, J = 1.2 Hz, 1H), 6.27 (t, J = 1.2 Hz, 1H), 4.92–4.81 (m, 8H), 2.90 (t, J = 6.8 Hz, 2H), 2.75 (br), 2.54 (s, 3H), 2.26 (t, J = 6.0 Hz, 2H), 2.07–2.00 (m, 2H). ^{13}C NMR (δ (ppm), $CDCl_3$, 100.65 MHz): 177.81, 167.96, 167.79, 156.69, 155.87, 155.03, 151.88, 150.85, 150.75, 149.51, 149.27, 148.35, 148.07, 143.34, 143.14, 141.40, 141.38, 140.43, 139.61, 131.77, 131.68, 130.76, 130.64, 128.48, 126.19, 124.79, 124.50, 124.31, 123.61, 122.45, 122.39, 121.19, 120.84, 120.50, 120.45, 116.88, 116.73, 109.56, 72.41, 70.51, 36.52, 35.05, 26.64, 21.49. MALDI-TOF-MS: m/z 1657.7 $[M-Cl]^+$.

IrL_{G2}: (Yield: 40%). ^{1}H NMR (δ (ppm), $CDCl_3$, 400 MHz): 8.71 (s, 1H), 8.61 (s, 1H), 8.09 (d, J = 7.6 Hz, 16H), 7.77 (s, 2H), 7.72–7.70 (m, 12H), 7.59 (d, J = 5.2 Hz, 2H), 7.47 (d, J = 8.4 Hz, 18H), 7.38–7.30 (m, 18H), 7.27–7.23 (m, 17H), 7.05 (d, J = 5.6 Hz, 1H), 6.95 (d, J = 5.6 Hz, 1H), 6.91 (d, J = 6.0 Hz, 1H), 6.86–6.77 (m, 3H), 6.75–6.69 (m, 8H), 6.18 (d, J = 7.2 Hz, 2H), 5.26 (s, 8H), 4.63–4.62 (m, 8H), 2.85 (t, J = 6.8 Hz, 2H), 2.51 (br), 2.47 (s, 3H), 2.25 (t, J = 6.4 Hz, 2H), 2.03–1.96 (m, 2H). ^{13}C NMR (δ (ppm), $CDCl_3$, 100.65 MHz): 177.85, 167.71, 167.52, 159.71, 156.58, 155.81, 154.98, 151.82, 150.81, 150.71, 149.84, 149.40, 149.14, 148.16, 147.87, 143.37, 143.18, 140.58, 140.37, 140.16, 140.14, 139.53, 131.67, 131.59, 130.61, 130.48, 128.34, 126.87, 126.11, 124.63, 124.58, 124.39, 124.20, 123.56, 122.28, 122.23, 121.22, 120.87, 120.42, 120.38, 117.05, 116.92, 109.94, 109.55, 107.38, 107.35, 101.90, 101.87, 73.10, 69.82, 69.11, 36.43, 34.97, 26.57, 21.41. MALDI-TOF-MS: m/z 2742.3 $[M]^+$.

IrL_{G3}: (Yield: 20%). ^{1}H NMR (δ (ppm), $CDCl_3$, 400 MHz): 8.74 (d, J = 3.2 Hz, 2H), 8.02 (d, J = 8.0 Hz, 31H), 7.73–7.17 (m, 129H), 6.96 (d, J = 5.2 Hz, 1H), 6.87–6.50 (m, 26H), 6.91 (m, 2H), 5.17 (s, 16H), 4.89 (s, 8H), 4.46 (s, 4H), 4.40 (s, 4H), 2.85 (t, J = 6.0 Hz, 2H), 2.42 (s, 3H), 2.37 (br), 2.30 (t, J = 6.4 Hz, 2H), 2.98–1.96 (m, 2H). ^{13}C NMR (δ (ppm), $CDCl_3$, 100.65 MHz): 177.23, 167.72, 167.44, 160.00, 159.62, 156.03, 155.69, 155.27, 151.96, 150.92, 149.97, 149.48, 149.11, 148.27, 147.94, 143.55, 143.32, 140.68, 140.39, 139.82, 139.78, 139.53, 139.04, 131.84, 131.67, 130.62, 130.45, 128.76, 128.45, 128.28, 126.88, 126.15, 125.31, 124.70, 124.29, 124.13, 123.59, 123.28, 123.14, 122.27, 121.33, 120.91, 120.41, 120.39, 116.96, 116.77, 113.12, 111.06, 109.60, 106.91, 102.02, 101.47, 73.11, 69.80, 69.73, 69.08, 35.63, 34.93, 26.16, 21.40. MALDI-TOF-MS: m/z 4917.0 $[M]^+$.

IrL_{G0}': (Yield: 83%). ^{1}H NMR (δ (ppm), $CDCl_3$, 400 MHz): 8.77 (d, J = 7.8 Hz, 2H), 7.86–7.82 (m, 2H), 7.74–7.69 (m, 4H), 7.55 (d, J = 8.0 Hz, 2H), 7.47–7.44 (m, 2H), 7.25–7.23 (m, H), 7.20–7.18 (m, H), 7.02–6.94 (m, 2H), 6.84–6.82 (m, 2H), 6.08 (s, 2H), 3.30 (br), 2.94 (t, J = 7.2 Hz, 2H), 2.60 (s, 3H), 2.35–2.28 (m, 2H), 2.12 (s, 6H), 2.09–2.04 (m, 2H). ^{13}C NMR (δ (ppm), $CDCl_3$, 100.65 MHz): 177.95, 167.80, 167.68, 156.21, 155.59, 155.25, 151.84, 150.77, 149.33, 148.29, 148.14, 140.80, 140.72, 140.66, 137.74, 137.70, 132.40, 132.36, 128.56, 128.20, 125.92, 125.55, 124.50, 124.46, 123.46, 123.42, 122.63, 122.49, 119.07, 118.96, 35.96, 34.80, 26.45, 21.71, 21.38. TOF-MS (ESI): Calcd. for $[M-Cl]^+$ 785.2468; found, 785.2475.

IrL_{G1}': (Yield: 60%). ^{1}H NMR (δ (ppm), $CDCl_3$, 400 MHz): 8.96 (s, 1H), 8.79 (s, 1H), 8.18 (d, J = 8.0 Hz, 8H), 7.73–7.72 (m, 2H), 7.60–7.58 (m, 2H), 7.52–7.42 (m, 20H), 7.35–7.31 (m, 10H), 7.07 (d, J = 5.2 Hz, 1H), 6.98 (d, J = 5.6 Hz, 1H), 6.88–6.64 (m, 9H), 6.49 (t, J = 6.8 Hz, 1H), 6.19 (s, 2H), 4.61–4.34 (m, 8H), 2.94 (br), 2.85 (t, J = 6.0 Hz, 2H), 2.55–2.41 (m, 5H), 2.07–2.04 (m, 2H). ^{13}C NMR (δ (ppm), $CDCl_3$, 100.65 MHz): 176.73, 167.09, 166.71, 155.55, 155.41, 155.36, 152.15, 150.84, 150.78, 149.55, 149.09, 148.17, 143.06, 142.84, 142.47, 142.41, 140.53, 140.51, 139.49, 139.19, 139.16, 137.66, 130.21, 129.94, 128.45, 128.16, 126.28, 126.01, 124.62, 124.35, 123.28, 122.80, 121.69, 120.59, 120.55, 120.50, 120.47, 119.12, 118.89, 109.78, 109.73, 72.69, 71.21, 34.84, 30.96, 25.74, 21.43. TOF-MS (ESI): Calcd. for $[M-Cl]^+$ 1657.5619; found, 1657.5631.

Acknowledgements

The financial support of this work from National Science Foundation of China (NSFC) under Project Nos. 20904038 and 21072218 is gratefully acknowledged.

Notes and references

1 M. A. Baldo, S. Lamansky, P. E. Burrows, M. E. Thompson and S. R. Forrest, *Appl. Phys. Lett.*, 1999, **75**, 4.
2 C. Adachi, M. A. Baldo, M. E. Thompson and S. R. Forrest, *J. Appl. Phys.*, 2001, **90**, 5048.
3 S. Lamansky, P. I. Djurovich, F. Abdel-Razzaq, S. Garon, D. L. Murphy and M. E. Thompson, *J. Appl. Phys.*, 2002, **92**, 1570.
4 J. P. Duan, P. P. Sun and C. H. Cheng, *Adv. Mater.*, 2003, **15**, 224.
5 A. Tsuboyama, H. Iwawaki, M. Furugori, T. Mukaide, J. Kamatani, S. Igawa, T. Moriyama, S. Miura, T. Takiguchi, S. Okada, M. Hoshino and K. Ueno, *J. Am. Chem. Soc.*, 2003, **125**, 12971.
6 S. G. Jung, Y. J. Kang, H. S. Kim, Y. H. Kim, C. L. Lee, J. J. Kim, S. K. Lee and S. K. Kwon, *Eur. J. Inorg. Chem.*, 2004, 3415.
7 Y. H. Song, S. J. Yeh, C. T. Chen, Y. Chi, C. S. Liu, J. K. Yu, Y. H. Hu, P. T. Chou, S. M. Peng and G. H. Lee, *Adv. Funct. Mater.*, 2004, **14**, 1221.
8 D. K. Rayabarapu, B. Paulose, J. P. Duan and C. H. Cheng, *Adv. Mater.*, 2005, **17**, 349.
9 K. K. W. Lo, C. K. Chung and N. Y. Zhu, *Chem.–Eur. J.*, 2003, **9**, 475.
10 K. K. W. Lo and J. S. Y. Lau, *Inorg. Chem.*, 2007, **46**, 700.
11 K. K. W. Lo, D. C. M. Ng and C. K. Chung, *Organometallics*, 2001, **20**, 4999.
12 K. K. W. Lo, K. Y. Zhang, S. K. Leung and M. C. Tang, *Angew. Chem., Int. Ed.*, 2008, **47**, 2213.
13 D. L. Ma, W. L. Wong, W. H. Chung, F. Y. Chan, P. K. So, T. S. Lai, Z. Y. Zhou, Y. C. Leung and K. Y. Wong, *Angew. Chem., Int. Ed.*, 2008, **47**, 3735.
14 S. K. Leung, K. Y. Kwok, K. Y. Zhang and K. K. W. Lo, *Inorg. Chem.*, 2010, **49**, 4984.
15 K. Y. Zhang, S. P. Y. Li, N. Y. Zhu, I. W. S. Or, M. S. H. Cheung, Y. W. Lam and K. K. W. Lo, *Inorg. Chem.*, 2010, **49**, 2530.
16 K. Y. Zhang, H. W. Liu, T. T. H. Fong, X. G. Chen and K. K. W. Lo, *Inorg. Chem.*, 2010, **49**, 5432.
17 T. Matsumoto, D. J. Taube, R. A. Periana, H. Taube and H. Yoshida, *J. Am. Chem. Soc.*, 2000, **122**, 7414.
18 R. M. Gao, D. G. Ho, B. Hernandez, M. Selke, D. Murphy, P. I. Djurovich and M. E. Thompson, *J. Am. Chem. Soc.*, 2002, **124**, 14828.
19 M. C. DeRosa, D. J. Hodgson, G. D. Enright, B. Dawson, C. E. B. Evans and R. J. Crutchley, *J. Am. Chem. Soc.*, 2004, **126**, 7619.
20 L. Huynh, Z. U. Wang, J. Yang, V. Stoeva, A. Lough, I. Manners and M. A. Winnik, *Chem. Mater.*, 2005, **17**, 4765.
21 S. M. Borisov and I. Klimant, *Anal. Chem.*, 2007, **79**, 7501.
22 M. L. Ho, F. M. Hwang, P. N. Chen, Y. H. Hu, Y. M. Cheng, K. S. Chen, G. H. Lee, Y. Chi and P. T. Chou, *Org. Biomol. Chem.*, 2006, **4**, 98.
23 M. L. Ho, Y. M. Cheng, L. C. Wu, P. T. Chou, G. H. Lee, F. C. Hsu and Y. Chi, *Polyhedron*, 2007, **26**, 4886.
24 M. Schmittel and H. W. Lin, *Inorg. Chem.*, 2007, **46**, 9139.
25 J. Brandel, M. Sairenji, K. Ichikawa and T. Nabeshima, *Chem. Commun.*, 2010, **46**, 3958.
26 Q. Zhao, S. Liu, M. Shi, F. Li, H. Jing, T. Yi and C. Huang, *Organometallics*, 2007, **26**, 5922.
27 Q. Zhao, F. Y. Li, S. J. Liu, M. X. Yu, Z. Q. Liu, T. Yi and C. H. Huang, *Inorg. Chem.*, 2008, **47**, 9256.
28 W. Goodall and J. A. G. Williams, *J. Chem. Soc., Dalton Trans.*, 2000, 2893.
29 H. L. Chen, Q. Zhao, Y. B. Wu, F. Y. Li, H. Yang, T. Yi and C. H. Huang, *Inorg. Chem.*, 2007, **46**, 11075.
30 N. Zhao, Y. H. Wu, L. X. Shi, Q. P. Lin and Z. N. Chen, *Dalton Trans.*, 2010, **39**, 8288.
31 H. Yersin, *Highly Efficient OLEDs with Phosphorescent Materials*, Wiley-VCH, 2008.
32 A. Endo, K. Suzuki, T. Yoshihara, S. Tobita, M. Yahiro and C. Adachi, *Chem. Phys. Lett.*, 2008, **460**, 155.
33 T. Sajoto, P. I. Djurovich, A. Tamayo, M. Yousufuddin, R. Bau, M. E. Thompson, R. J. Holmes and S. R. Forrest, *Inorg. Chem.*, 2005, **44**, 7992.
34 T. H. Kwon, H. S. Cho, M. K. Kim, J. W. Kim, J. J. Kim, K. H. Lee, S. J. Park, I. S. Shin, H. Kim, D. M. Shin, Y. K. Chung and J. I. Hong, *Organometallics*, 2005, **24**, 1578.
35 M. K. Nazeeruddin, R. Humphry-Baker, D. Berner, S. Rivier, L. Zuppiroli and M. Graetzel, *J. Am. Chem. Soc.*, 2003, **125**, 8790.
36 Q. Zhao, S. J. Liu, M. Shi, C. M. Wang, M. X. Yu, L. Li, F. Y. Li, T. Yi and C. H. Huang, *Inorg. Chem.*, 2006, **45**, 6152.
37 G. F. Blackburn, H. P. Shah, J. H. Kenten, J. Leland, R. A. Kamin, J. Link, J. Peterman, M. J. Powell, A. Shah, D. B. Talley, S. K. Tyagi, E. Wilkins, T. G. Wu and R. J. Massey, *Clin. Chem.*, 1991, **37**, 1534.
38 I. Hemmila and V. Laitala, *J. Fluoresc.*, 2005, **15**, 529.
39 J. L. Yuan and G. L. Wang, *J. Fluoresc.*, 2005, **15**, 559.
40 SunaTech Inc. Website: http://www.sunatech.com.
41 S. Zanarini, E. Rampazzo, S. Bonacchi, R. Juris, M. Marcaccio, M. Montalti, F. Paolucci and L. Prodi, *J. Am. Chem. Soc.*, 2009, **131**, 14208.
42 T. Förster, *Discuss. Faraday Soc.*, 1959, **27**, 7.
43 H. P. Yu, S. M. Zain, I. V. Eigenbrot and D. Phillips, *Chem. Phys. Lett.*, 1993, **202**, 141.
44 F. Loiseau, S. Campagna, A. Hameurlaine and W. Dehaen, *J. Am. Chem. Soc.*, 2005, **127**, 11352.
45 B. L. Li, L. Wu, Y. M. He and Q. H. Fan, *Dalton Trans.*, 2007, 2048.
46 T. H. Kwon, M. K. Kim, J. Kwon, D. Y. Shin, S. J. Park, C. L. Lee, J. J. Kim and J. I. Hong, *Chem. Mater.*, 2007, **19**, 3673.
47 T. H. Kwon, H. J. Kim and J. I. Hong, *Chem.–Eur. J.*, 2008, **14**, 9613.
48 T. H. Kwon, J. Kwon and J. I. Hong, *J. Am. Chem. Soc.*, 2008, **130**, 3726.
49 K. R. J. Thomas, A. L. Thompson, A. V. Sivakumar, C. J. Bardeen and S. Thayumanavan, *J. Am. Chem. Soc.*, 2005, **127**, 373.
50 A. Nantalaksakul, D. R. Reddy, C. J. Bardeen and S. Thayumanavan, *Photosynth. Res.*, 2006, **87**, 133.
51 S. Serroni, S. Campagna, A. Juris, M. Venturi, V. Balzani and G. Denti, *Gazz. Chim. Ital.*, 1994, **124**, 423.
52 G. T. Hermanson, *Bioconjugate Techniques*, 2nd Ed., Academic Press, 2008.
53 M. Nonoyama, *Bull. Chem. Soc. Jpn.*, 1974, **47**, 767.
54 N. D. McClenaghan, R. Passalacqua, F. Loiseau, S. Campagna, B. Verheyde, A. Hameurlaine and W. Dehaen, *J. Am. Chem. Soc.*, 2003, **125**, 5356.
55 S. C. Lo, E. B. Namdas, P. L. Burn and I. D. W. Samuel, *Macromolecules*, 2003, **36**, 9721.
56 U. Hahn, F. Vögtle, G. De Paoli, M. Staffilani and L. De Cola, *Eur. J. Inorg. Chem.*, 2009, 2639.
57 M. Zhou and J. Roovers, *Macromolecules*, 2001, **34**, 244.
58 J. Q. Ding, J. Gao, Y. X. Cheng, Z. Y. Xie, L. X. Wang, D. G. Ma, X. B. Jing and F. S. Wang, *Adv. Funct. Mater.*, 2006, **16**, 575.
59 J. R. Lakowicz, *Principles of Fluorescence Spectroscopy*, the Third Edition, Springer, 2006.
60 The simulated molecular structures were obtained by minimizing energy calculations under MM2 method provided by ChemBio3D Ultra (12.0 edition).
61 S. Campagna, F. Puntoriero, F. Nastasi, G. Bergamini and V. Balzani, *Top. Curr. Chem.*, 2007, **280**, 117.
62 J. D. Slinker, A. A. Gorodetsky, M. S. Lowry, J. J. Wang, S. Parker, R. Rohl, S. Bernhard and G. G. Malliaras, *J. Am. Chem. Soc.*, 2004, **126**, 2763.
63 C. Schaffner-Hamann, A. von Zelewsky, A. Barbieri, F. Barigelletti, G. Muller, J. P. Riehl and A. Neels, *J. Am. Chem. Soc.*, 2004, **126**, 9339.
64 A. Ruggi, M. B. Alonso, D. N. Reinhoudt and A. H. Velders, *Chem. Commun.*, 2010, **46**, 6726.
65 S. J. Zhang, M. Hosaka, T. Yoshihara, K. Negishi, Y. Iida, S. Tobita and T. Takeuchi, *Cancer Res.*, 2010, **70**, 4490.
66 A. L. Medina-Castillo, J. F. Fernandez-Sanchez, C. Klein, M. K. Nazeeruddin, A. Segura-Carretero, A. Fernandez-Gutierrez, M. Graetzel and U. E. Spichiger-Keller, *Analyst*, 2007, **132**, 929.
67 J. Issberner, F. Vögtle, L. DeCola and V. Balzani, *Chem.–Eur. J.*, 1997, **3**, 706.
68 M. Plevoets, F. Vögtle, L. De Cola and V. Balzani, *New J. Chem.*, 1999, **23**, 63.
69 R. P. Brinas, T. Troxler, R. M. Hochstrasser and S. A. Vinogradov, *J. Am. Chem. Soc.*, 2005, **127**, 11851.
70 E. Baranoff, S. Suarez, P. Bugnon, H. J. Bolink, C. Klein, R. Scopelliti, L. Zuppiroli, M. Gratzel and M. K. Nazeeruddin, *ChemSusChem*, 2009, **2**, 305.